

Fidelity susceptibility and long-range correlation in the Kitaev honeycomb model

Shuo Yang,^{1,2} Shi-Jian Gu,^{1,*} Chang-Pu Sun,² and Hai-Qing Lin¹

¹*Department of Physics and ITP, The Chinese University of Hong Kong, Hong Kong, China*

²*Institute of Theoretical Physics, Chinese Academy of Sciences, Beijing, 100080, China*

(Dated: January 28, 2019)

We study exactly both the ground-state fidelity susceptibility and bond-bond correlation function in the Kitaev honeycomb model. Our results show that the fidelity susceptibility can be used to identify the topological phase transition from a gapped A phase with Abelian anyon excitations to a gapless B phase with non-Abelian anyon excitations. We also find that the bond-bond correlation function decays exponentially in the gapped phase, while algebraically in the gapless phase. For the former case, the correlation length is found to be $1/\xi = 2 \sinh^{-1}[\sqrt{2J_z - 1}/(1 - J_z)]$, which diverges around the critical point $J_z = (1/2)^+$.

PACS numbers: 03.67.-a, 64.60.-i, 05.30.Pr, 75.10.Jm

I. INTRODUCTION

Quite recently, a great deal of effort [1, 2, 3, 4, 5, 6, 7, 8, 9, 10, 11, 12, 13, 14, 15, 16] has been devoted to the role of fidelity, a concept borrowed from quantum information theory [17], in quantum phase transitions (QPTs) [18]. The motivation is quite obvious. Since the fidelity is a measure of similarity between two states, the change of the ground state structure around the quantum critical point should result in a dramatic change in the fidelity across the critical point. Such a fascinating prospect has been demonstrated in many correlated systems. For example, in one-dimensional XY model, fidelity shows a narrow trough at the phase transition point [2]. Similar properties were also found in fermionic [3] and bosonic systems [4]. The advantage of fidelity lies that, since the fidelity is a space geometrical quantity, no priori knowledge of order parameter and symmetry-breaking is required in the studies of QPTs.

Nevertheless, the properties of the fidelity is mainly determined by its leading term [7, 8], i.e., its second derivative with respect to the driving parameter (or the so-called fidelity susceptibility [8]). According to the standard perturbation method, it has been shown that the fidelity susceptibility actually is equivalent to the structure factor (fluctuation) of the driving term in the Hamiltonian [8]. For example, if we focus on the thermal phase transitions and choose the temperature as driving parameter, the fidelity susceptibility, extracted from the mixed state fidelity between two thermal states [6], is simply the specific heat [7, 8]. From this point of view, the fidelity approach to QPTs seems still under the framework of the correlation functions approach, which is intrinsically related to the local order parameter.

However, some systems cannot be described in the framework built on the local order parameter. This might be due to the absence of preexistent symmetry in the

Hamiltonian, such as topological phase transition [19] and Kosterlitz-Thouless phase transition [20]. For the latter, since the transition is of infinite-order, it has already been pointed out that the fidelity might fail to identify the phase transition point [8, 11]. Therefore, it is an interesting issue to address the role of fidelity in studying the topological phase transition.

On the other hand, the Kitaev honeycomb model was first introduced by Kitaev in search of topological order and anyonic statistics. The model is associated with a system of $1/2$ spins which are located at the vertices of a honeycomb lattice. Each spin interacts with three nearest neighbored spins through three types of bonds, called “ $x(y, z)$ -bonds” depending on their direction. The model Hamiltonian [21] is as follows:

$$\begin{aligned} H &= -J_x \sum_{x\text{-bonds}} \sigma_j^x \sigma_k^x - J_y \sum_{y\text{-bonds}} \sigma_j^y \sigma_k^y - J_z \sum_{z\text{-bonds}} \sigma_j^z \sigma_k^z, \\ &= -J_x H_x - J_y H_y - J_z H_z. \end{aligned} \quad (1)$$

where j, k denote two ends of the corresponding bond, and J_a, σ^a ($a = x, y, z$) are coupling constants and Pauli matrixes respectively. Such a model is rather artificial. However, its potential application in the topological quantum computation placed it in one of research focus in recent years [21, 22, 23, 24, 25, 26, 27, 28, 29, 30, 31, 32].

The ground state of the Kitaev honeycomb model consists of two phases, i.e., a gapped A phase with Abelian anyon excitations and a gapless B phase with non-Abelian anyon excitations. The transition has been studied by various approaches. For example, it has been shown that a kind of long range order exists in the dual space [26], such that basic concepts of Landau’s theory of continuous phase transitions might still be applied. In real space, however, the spin-spin correlation functions vanishes rapidly with the increasing of distance between two spins. Therefore, the transition between the two phases is believed to be of topological type due to the absence of local order parameter in real space [21].

In this work, we *firstly* try to investigate the topological QPT occurred in the ground state of the Kitaev honeycomb model in terms of the fidelity susceptibility.

*Electronic address: sjgu@phy.cuhk.edu.hk

We find that the fidelity susceptibility can be used to identify the topological phase transition from a gapped phase with Abelian anyon excitations to another gapless phase with non-Abelian anyon excitations. Various scaling and critical exponents of the fidelity susceptibility around the critical points are obtained through the standard finite-size scaling analysis. *These observations from the fidelity approach are a little surprising.* Earlier thought is that the fidelity susceptibility, which is a kind of structure factor obtained by a combination of correlation functions, can hardly be related to the topological phase transition, since the latter cannot be described by the correlation functions of local operators. So our *second* motivation followed from the first one is to study the dominant correlation function appeared in the definition of the fidelity susceptibility, i.e., the bond-bond correlation function. We find the correlation function decays algebraically in the gapless phase, while exponentially in the gapped phase. For the latter, the correlation length takes the form $1/\xi = 2 \sinh^{-1}[\sqrt{2J_z - 1}/(1 - J_z)]$ along a given evolution line. Therefore, the divergence of the correlation length around the critical point $J_z = (1/2)^+$ is also a signature of the QPT.

We organize our work as follows. In section II, we introduce briefly the definition of the fidelity susceptibility in the Hamiltonian's parameter space, then we diagonalize the Hamiltonian based on Kitaev's approaches and obtain the explicit forms of the Riemann metric tensor, from which the fidelity susceptibility along any direction can be obtained. The critical and scaling behavior of the fidelity susceptibility are also studied numerically. In section III, we explicitly calculate the bond-bond correlation functions in the both phases. Its long range behavior and the correlation length in the gapped phase are studied both analytically and numerically. Section IV includes a brief summary.

II. FIDELITY SUSCEPTIBILITY IN THE GROUND STATE

To study the fidelity susceptibility, we notice that the structure of the parameter space of the Hamiltonian (1) is three dimensional. In this space, we can always let the ground state of the Hamiltonian evolves along a certain path in the parameter space, i.e.,

$$J_a = J_a(\lambda), \quad (2)$$

where λ plays a kind of driving parameter along the evolution line. We then extend the definition of fidelity to this arbitrary line in high-dimensional space. Following Ref. [2], the fidelity is defined as the overlap between two ground state

$$F = |\langle \Psi_0(\lambda) | \Psi_0(\lambda + \delta\lambda) \rangle|, \quad (3)$$

where $\delta\lambda$ is the magnitude of a small displacement along the tangent direction at λ . Then the fidelity susceptibil-

ity along this line can be calculated as

$$\chi_F = \lim_{\delta\lambda \rightarrow 0} \frac{-2 \ln F_i}{\delta\lambda^2} = \sum_{ab} g_{ab} n^a n^b, \quad (4)$$

where $n^a = \partial J_a / \partial \lambda$ denotes the tangent unit vector at the given point, g_{ab} is the Riemann metric tensor introduced by Zanardi, Giorda, and Cozzini[7]. For the present model, we have

$$g_{ab} = \sum_n \frac{\langle \Psi_n(\lambda) | H_a | \Psi_0(\lambda) \rangle \langle \Psi_0(\lambda) | H_b | \Psi_n(\lambda) \rangle}{(E_n - E_0)^2}, \quad (5)$$

where $|\Psi_n(\lambda)\rangle$ is the eigenstate of the Hamiltonian with energy E_n . Clearly, g_{ab} does not depend on a specific path along which the system evolves. However, once g_{ab} are obtained, the fidelity susceptibility is just a simple combination of g_{ab} together with a unit vector which defines the direction of system evolution in the parameter space.

According to Kitaev [21], the Hamiltonian (1) can be diagonalized exactly by introducing Majorana fermion operators to represent Pauli operators as

$$\sigma^x = ib^x c, \quad \sigma^y = ib^y c, \quad \sigma^z = ib^z c, \quad (6)$$

where Majorana operators satisfy $A^2 = 1$, $AB = -BA$ for $A, B \in \{b^x, b^y, b^z, c\}$ and $A \neq B$, and also $b^x b^y b^z c |\psi\rangle = |\psi\rangle$ to ensure the commutation relations of spin operators. Then the Hamiltonian can be written as

$$H = \frac{i}{2} \sum_{j,k} \hat{u}_{jk} J_{a_{jk}} c_j c_k. \quad (7)$$

Since the operators $\hat{u}_{jk} = ib_j^{a_{jk}} b_k^{a_{jk}}$ satisfy $[\hat{u}_{jk}, H] = 0$, $[\hat{u}_{jk}, \hat{u}_{ml}] = 0$, and $\hat{u}_{jk}^2 = 1$, they can be regarded as the generators of Z_2 symmetry group. Therefore, the whole Hilbert space can be decomposed into common eigenspaces of \hat{u}_{jk} , each subspace is characterized by a group of $u_{jk} = \pm 1$. The spin model is transformed to a quadratic Majorana fermionic Hamiltonian

$$H = \frac{i}{2} \sum_{j,k} u_{jk} J_{a_{jk}} c_j c_k. \quad (8)$$

Here we only restrict ourselves to the vortex free subspace with translational invariant, i.e., all $u_{jk} = 1$. After Fourier transformation, we get the Hamiltonian of a unit cell in the momentum representation [21]

$$H = \sum_{\mathbf{q}} \begin{pmatrix} a_{-\mathbf{q},1} \\ a_{-\mathbf{q},2} \end{pmatrix}^T \begin{pmatrix} 0 & if(\mathbf{q}) \\ -if(\mathbf{q})^* & 0 \end{pmatrix} \begin{pmatrix} a_{\mathbf{q},1} \\ a_{\mathbf{q},2} \end{pmatrix}, \quad (9)$$

where $\mathbf{q} = (q_x, q_y)$,

$$a_{\mathbf{q},\gamma} = \frac{1}{\sqrt{2L^2}} \sum_{\mathbf{r}} e^{-i\mathbf{q}\cdot\mathbf{r}} c_{\mathbf{r},\gamma}, \quad (10)$$

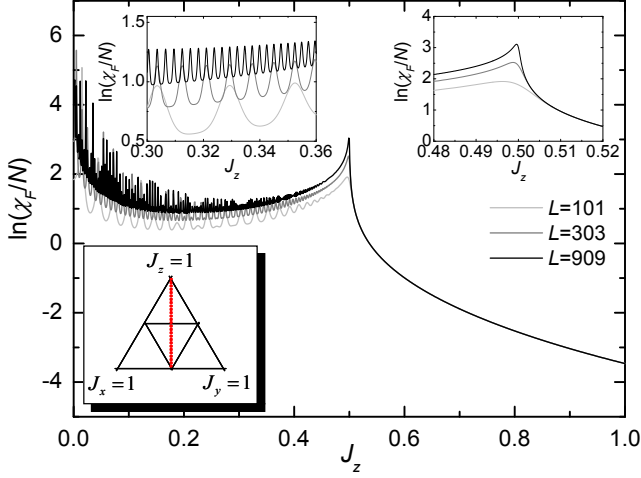


FIG. 1: (color online) The fidelity susceptibility as a function of J_z along the dashed line shown in the triangle for various system sizes $L = 101, 303, 909$. Both up insets correspond to enlarged picture of two small portions.

\mathbf{r} refers to the coordinate of a unit cell while γ to a position type inside the cell, and

$$\begin{aligned} f(\mathbf{q}) &= \epsilon_{\mathbf{q}} + i\Delta_{\mathbf{q}}, \\ \epsilon_{\mathbf{q}} &= J_x \cos q_x + J_y \cos q_y + J_z, \\ \Delta_{\mathbf{q}} &= J_x \sin q_x + J_y \sin q_y. \end{aligned} \quad (11)$$

Here, we set L to be an odd integer, then the system size is $N = 2L^2$. The momenta take

$$q_{x(y)} = \frac{2n\pi}{L}, n = -\frac{L-1}{2}, \dots, \frac{L-1}{2}. \quad (12)$$

The above Hamiltonian can be rewritten by some fermionic operators as

$$H = \sum_{\mathbf{q}} \sqrt{\epsilon_{\mathbf{q}}^2 + \Delta_{\mathbf{q}}^2} \left(C_{\mathbf{q},1}^\dagger C_{\mathbf{q},1} - C_{\mathbf{q},2}^\dagger C_{\mathbf{q},2} \right). \quad (13)$$

Therefore, we have the ground state

$$\begin{aligned} |\Psi_0\rangle &= \prod_{\mathbf{q}} C_{\mathbf{q},2}^\dagger |0\rangle \\ &= \prod_{\mathbf{q}} \frac{1}{\sqrt{2}} \left(\frac{\sqrt{\epsilon_{\mathbf{q}}^2 + \Delta_{\mathbf{q}}^2}}{\Delta_{\mathbf{q}} + i\epsilon_{\mathbf{q}}} a_{-\mathbf{q},1} + a_{-\mathbf{q},2} \right) |0\rangle, \end{aligned} \quad (14)$$

with the ground state energy

$$E_0 = - \sum_{\mathbf{q}} \sqrt{\epsilon_{\mathbf{q}}^2 + \Delta_{\mathbf{q}}^2}. \quad (15)$$

The fidelity of the two ground states at λ and λ' can be obtained as

$$\begin{aligned} F^2 &= \prod_{\mathbf{q}} \frac{1}{2} \left(1 + \frac{\Delta_{\mathbf{q}} \Delta'_{\mathbf{q}} + \epsilon_{\mathbf{q}} \epsilon'_{\mathbf{q}}}{E_{\mathbf{q}} E'_{\mathbf{q}}} \right), \\ &= \prod_{\mathbf{q}} \cos^2(\theta_{\mathbf{q}} - \theta'_{\mathbf{q}}). \end{aligned} \quad (16)$$

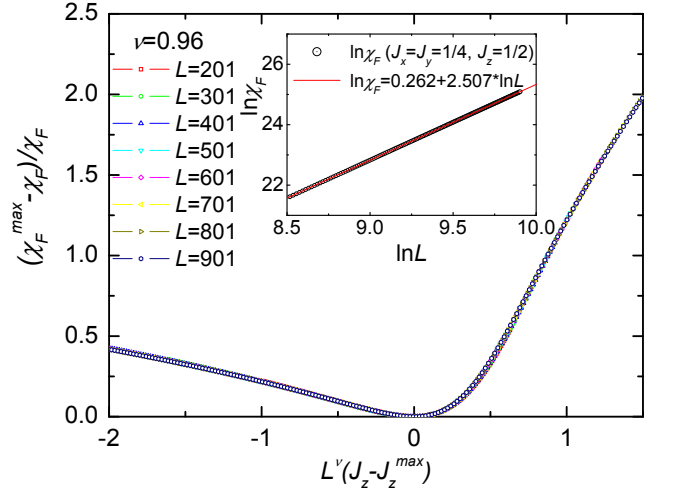


FIG. 2: (color online) The finite size scaling analysis is performed for the case of power-law divergence for systems sizes $L = 201, 301, \dots, 901$. The fidelity susceptibility, considered as a function of system size and driving parameter is a function of $L^\nu (J_z - J_z^{\max})$ only, has the critical exponent $\nu = 0.96$.

with

$$\begin{aligned} \cos(2\theta_{\mathbf{q}}) &= \frac{\epsilon_{\mathbf{q}}}{E_{\mathbf{q}}}, \sin(2\theta_{\mathbf{q}}) = \frac{\Delta_{\mathbf{q}}}{E_{\mathbf{q}}}, \\ \cos(2\theta'_{\mathbf{q}}) &= \frac{\epsilon'_{\mathbf{q}}}{E'_{\mathbf{q}}}, \sin(2\theta'_{\mathbf{q}}) = \frac{\Delta'_{\mathbf{q}}}{E'_{\mathbf{q}}}. \end{aligned} \quad (17)$$

The Riemann metric tensor can be expressed as

$$g^{ab} = \sum_{\mathbf{q}} \left(\frac{\partial \theta_{\mathbf{q}}}{\partial J_a} \right) \left(\frac{\partial \theta_{\mathbf{q}}}{\partial J_b} \right), \quad (18)$$

where

$$\begin{aligned} \frac{\partial(2\theta_{\mathbf{q}})}{\partial J_x} &= \frac{J_z \sin q_x + J_y \sin(q_x - q_y)}{\epsilon_{\mathbf{q}}^2 + \Delta_{\mathbf{q}}^2} \cdot \frac{\Delta_{\mathbf{q}}}{|\Delta_{\mathbf{q}}|}, \\ \frac{\partial(2\theta_{\mathbf{q}})}{\partial J_y} &= -\frac{J_x \sin(q_x - q_y) - J_z \sin q_y}{\epsilon_{\mathbf{q}}^2 + \Delta_{\mathbf{q}}^2} \cdot \frac{\Delta_{\mathbf{q}}}{|\Delta_{\mathbf{q}}|}, \\ \frac{\partial(2\theta_{\mathbf{q}})}{\partial J_z} &= -\frac{J_x \sin q_x + J_y \sin q_y}{\epsilon_{\mathbf{q}}^2 + \Delta_{\mathbf{q}}^2} \cdot \frac{\Delta_{\mathbf{q}}}{|\Delta_{\mathbf{q}}|}. \end{aligned} \quad (19)$$

Clearly, with these equations, we can in principle calculate the fidelity susceptibility along any direction in the parameter space according to Eq. (4). Here, we would like to point out that the same results can be obtained from the generalized Jordan-Wigner transformation used firstly by Feng, Zhang, and Xiang[26].

Following Kitaev [21], we restrict our studies on the plane $J_x + J_y + J_z = 1$ (see the large triangle in Fig. 1). According to his results, the plane consists of two phases, i.e., a gapped A phase with Abelian anyon excitations and a gapless B phase with non-Abelian excitations. The two phases are separated by three transition lines, i.e. $J_x = 1/2$, $J_y = 1/2$, and $J_z = 1/2$ which form a small triangle of the B phase.

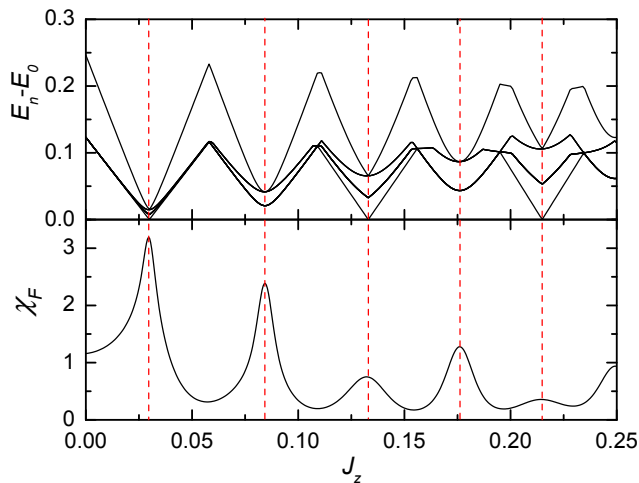


FIG. 3: (color online) The fidelity susceptibility and a few low-lying excitations as a function of J_z in a small portion of the evolution line for system size $L = 51$.

Generally, we can define an arbitrary evolution line on the plane. Without loss of generality, we first choose the line as $J_x = J_y$ (see the dashed line in the triangle of Fig. 1). Then the fidelity susceptibility along this line can be simplified as

$$\chi_F = \frac{1}{16} \sum_{\mathbf{q}} \left[\frac{\sin q_x + \sin q_y}{\epsilon_{\mathbf{q}}^2 + \Delta_{\mathbf{q}}^2} \right]^2. \quad (20)$$

The numerical results of different system sizes are shown in Fig. 1. First of all, the fidelity susceptibility per site, i.e. χ_F/N diverges quickly with increasing system size around the critical point $J_z = 1/2$. This property is similar to the fidelity susceptibility in other systems, such as the one-dimensional Ising chain [2] and the asymmetric Hubbard model[12]. Secondly, χ_F/N is an intensive quantity in the A phase ($J_z > 1/2$), while in the B phase, the fidelity susceptibility also diverges with increasing system size. Thirdly, the fidelity susceptibility shows many peaks in the B phase, the number of peaks linearly increases with the system size L (see the left-up inset of Fig. 1). The new phenomena of fidelity susceptibility per site in B phase are not found in other systems previously, so that they are rather impressive.

To study the scaling behavior of the fidelity susceptibility around the critical point, we perform finite scaling analysis. Since the fidelity susceptibility in the A phase is an intensive quantity, the fidelity susceptibility in the thermodynamic limit, scales like [12]

$$\frac{\chi_F}{N} \propto \frac{1}{|J_z - J_z^c|^\alpha}. \quad (21)$$

around $J_z^c = 1/2$. Meanwhile, the maximum point of χ_F at $J_z = J_z^{\max}$ for a finite sample behavior like

$$\frac{\chi_F}{N} \propto L^\mu, \quad (22)$$

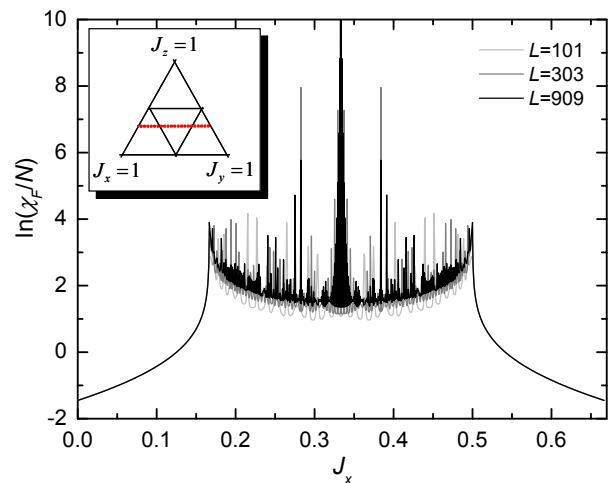


FIG. 4: (color online) The fidelity susceptibility as a function of $J_x = 2/3 - J_y$ along the dashed line shown in the triangle for various system sizes $L = 101, 303, 909$.

with $\mu = 0.507 \pm 0.0001$ (see the inset of Fig. 2). According to the scaling ansatz, the rescaled fidelity susceptibility around its maximum point at J_z^{\max} is just a simple function of the rescaled driving parameter, i.e.,

$$\frac{\chi_F^{\max} - \chi_F}{\chi_F} = f[L^\nu (J_z - J_z^{\max})]. \quad (23)$$

where $f(x)$ is a universal scaling function and does not depend on the system size, and ν is the critical exponent. The function $f(x)$ is shown in Fig. 2. Clearly, the rescaled fidelity susceptibility of various system sizes fall onto a single line for a specific $\nu = 0.96 \pm 0.005$. Then the critical exponent α can be obtained as

$$\alpha = \frac{\mu}{\nu} = 0.528 \pm 0.001. \quad (24)$$

One of the most interesting observations is that a huge number of peaks appear in the B phase. Scaling analysis manifests that the number of peaks is proportional to the system size. Physically, the peak means that the ground state can not adiabatically evolve from one side of the peak to the other side easily because the two ground states have distinct features. From this point of view, the ground state in the B phase might be stable to the adiabatic perturbation. Moreover, the existence of many peaks can also be reflected from the reconstruction of the energy spectra. For this purpose, we choose a small portion of evolution line and plot both the fidelity susceptibility and a few low-lying excitations in Fig. 3. Since the fidelity is inversely proportional to the energy gap [Eq. (5)], the location of each peak corresponds to a gap minimum.

Similarly, we can also choose the system evolution line as $J_z = 1/3$, the fidelity susceptibility then takes the

form

$$\chi_F = \frac{1}{36} \sum_{\mathbf{q}} \left[\frac{(\sin q_x - \sin q_y) + 2 \sin(q_x - q_y)}{\epsilon_{\mathbf{q}}^2 + \Delta_{\mathbf{q}}^2} \right]^2. \quad (25)$$

The numerical results for this case are shown in Fig. 4. The results are similar to previous cases qualitatively. In the B phase, there still exist many peaks. Both the number and the magnitude of the peaks increase with the system size. While in the A phase, the fidelity susceptibility becomes an intensive quantity.

III. LONG-RANGE CORRELATION AND FIDELITY SUSCEPTIBILITY

Follow You, *etal* [8], the fidelity susceptibility is a combination of correlation function. Precisely, for a general Hamiltonian

$$H = H_0 + \lambda H_I, \quad (26)$$

the fidelity susceptibility can be calculated as

$$\chi_F = \int \tau \left[\langle \Psi_0 | H_I(\tau) H_I(0) | \Psi_0 \rangle - \langle \Psi_0 | H_I | \Psi_0 \rangle^2 \right] d\tau, \quad (27)$$

with τ being the imaginary time and

$$H_I(\tau) = e^{H(\lambda)\tau} H_I e^{-H(\lambda)\tau}.$$

Therefore, the divergence of the fidelity susceptibility at the critical point implies the existence of the long-range correlation function. Without loss of generality, if we still restrict ourselves on the plane $J_x + J_y + J_z = 1$ and choose J_z ($J_x = J_y$) as driving parameter, the bond-bond correlation function defined as

$$C(\mathbf{r}_1, \mathbf{r}_2) = \langle \sigma_{\mathbf{r}_1,1}^z \sigma_{\mathbf{r}_1,2}^z \sigma_{\mathbf{r}_2,1}^z \sigma_{\mathbf{r}_2,2}^z \rangle - \langle \sigma_{\mathbf{r}_1,1}^z \sigma_{\mathbf{r}_1,2}^z \rangle \langle \sigma_{\mathbf{r}_2,1}^z \sigma_{\mathbf{r}_2,2}^z \rangle. \quad (28)$$

Here the subscripts $\mathbf{r}_1, 1$ and $\mathbf{r}_1, 2$ denote two ends of the single z -bond at $\mathbf{r}_1 = (x, y)$. In the vortex free case, through Eq. (6), (10), and (14), the spin operators $\sigma_{\mathbf{r}_1,1}^z \sigma_{\mathbf{r}_1,2}^z$ can be expressed in the form of fermion operators. So we finally get

$$\langle \sigma_{\mathbf{r}_1,1}^z \sigma_{\mathbf{r}_1,2}^z \rangle = \langle \sigma_{\mathbf{r}_2,1}^z \sigma_{\mathbf{r}_2,2}^z \rangle = \frac{1}{N} \sum_{\mathbf{q}} \frac{\epsilon_{\mathbf{q}}}{E_{\mathbf{q}}} \quad (29)$$

and

$$\begin{aligned} & \langle \Psi_0 | \sigma_{\mathbf{r}_1,1}^z \sigma_{\mathbf{r}_1,2}^z \sigma_{\mathbf{r}_2,1}^z \sigma_{\mathbf{r}_2,2}^z | \Psi_0 \rangle \\ &= \frac{1}{N^2} \sum_{\mathbf{q}, \mathbf{q}'} \{ \cos[(\mathbf{q} - \mathbf{q}')(\mathbf{r}_1 - \mathbf{r}_2)] - 1 \} \\ & \times \frac{(\Delta_{\mathbf{q}} \Delta_{\mathbf{q}'} - \epsilon_{\mathbf{q}} \epsilon_{\mathbf{q}'})}{E_{\mathbf{q}} E_{\mathbf{q}'}} \end{aligned} \quad (30)$$

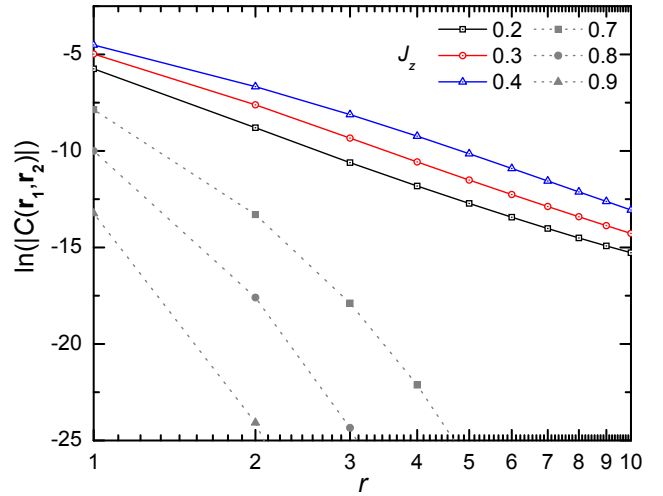


FIG. 5: (color online) The bond-bond correlation function as a function of distance r for various J_z and a finite sample of $L = 100$, where $\mathbf{r}_1 - \mathbf{r}_2 = (r, r)$. Downward peaks in top lines are due to zero-point crossing.

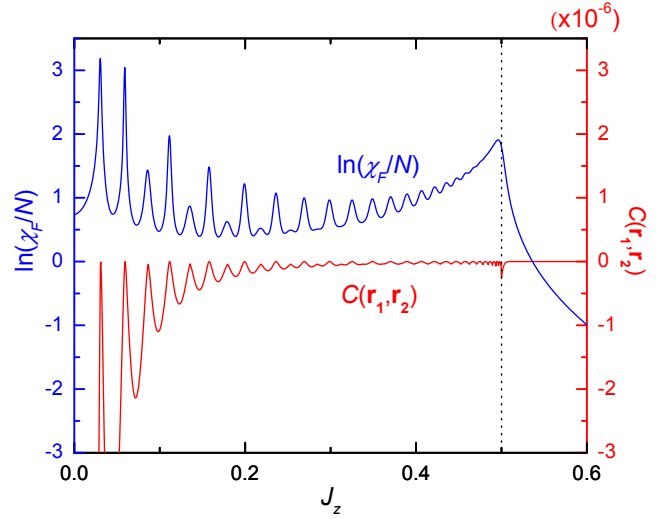


FIG. 6: (color online) The fidelity susceptibility and the correlation function at $\mathbf{r}_1 - \mathbf{r}_2 = (L/2, L/2)$ as a function of J_z for a finite sample of $L = 100$.

with $\mathbf{q} \neq \mathbf{q}'$ and $\mathbf{r}_1 \neq \mathbf{r}_2$. The same results can also be obtained by using the Jordan-Wigner transformation method [26, 27].

We show the dependence of the correlation function Eq. (28) on the distance for a finite sample of $L = 100$ in Fig. 5. Obviously, the lines can be divided into two groups. In the gapless phase ($J_z < 1/2$), the correlation function decays algebraically, while in gapped phase ($J_z > 1/2$), it decays exponentially. If $J_z < 1/2$, the denominator in Eq. (30) has two zero points, which are of order $1/N$ in large N limit. Their contribution makes the summation to be finite in the thermodynamic limit. Then using the method of stationary phase, we can eval-

uate the exponents of the correlation function at long distance to be 4, i.e.,

$$C(\mathbf{r}_1, \mathbf{r}_2) \propto \frac{1}{|\mathbf{r}_1 - \mathbf{r}_2|^4}. \quad (31)$$

From Fig. 5, the average slope of the top three lines around $r = 10$ are estimated to be 4.05, which is slightly different from 4. Nevertheless, we would rather interpret the difference due to both the finite size effects and numerical error. On the other hand, if $J_z > 1/2$, the phase is gapped and the denominator in Eq. (30) does not have any zero point on real axis. Therefore, the whole summation is strongly suppressed except for the case of small $|\mathbf{r}_1 - \mathbf{r}_2|$, whose range defines actually the correlation length. In order to evaluate the correlation, we need to extending the integrand (in the thermodynamic limit) in Eq. (30) to the whole complex plane, where we can find two singular points. Use the steepest decent method, we can evaluate the correlation length to be

$$\frac{1}{\xi} = 2 \sinh^{-1} \frac{\sqrt{2J_z - 1}}{1 - J_z}. \quad (32)$$

Obviously, the correlation length becomes divergent as $J_z \rightarrow 0.5^+$. This property can be also used to signal the QPT occurred in the Kitaev honeycomb model besides the fidelity and Chern number [21]. The correlation length we obtained is the same as that of the string operators [27], which, however, is a non-local operator.

Though it is not easy to calculate the fidelity susceptibility from the correlation function directly due to the dynamic term in Eq. (27), our conjecture is confirmed for the present model. That is the divergence of the fidelity susceptibility is related to the long-range correlations. Fig. 6 is illustrative. The correlation function at $\mathbf{r}_1 - \mathbf{r}_2 = (L/2, L/2)$, in despite of its smallness, keeps nonzero in the region $J_z < 1/2$, while vanishes in $J_z > 1/2$. For the former, the oscillating structure of both lines meet with each other.

IV. SUMMARY AND DISCUSSION

In summary, we have studied the critical behavior of the fidelity susceptibility where a topological phase transition occurred in the honeycomb Kitaev model. Though no symmetry breaking exists and no local order parameter in real space can be used to describe the transition, the fidelity susceptibility definitely can witness the transition point. We found that the fidelity susceptibility per site is an intensive quantity in the gapped phase, while in the gapless phase, the huge number of peaks reflects frequent spectra reconstruction along the evolution line. We also studied various scaling and critical exponents of the fidelity susceptibility around the critical points.

Based on the conclusion from the fidelity, we further studied the bond-bond correlation function in both phase. We found that bond-bond correlation function, which plays a dominant role in the expression of the fidelity susceptibility, decays exponentially in the gapped phase, while algebraically in the gapless phase. Both the critical exponents of the correlation function in the gapless phase and the correlation length in the gapped phase are calculated numerical and analytically. Therefore, besides the topological nature of the Kitaev honeycomb model, say Chern number, we found that both the fidelity susceptibility and the bond-bond correlation functions can be used to witness the QPT in the model.

Note added. After finishing this work, we noticed that a work on the fidelity per site in stead of fidelity susceptibility in the similar model appeared[33].

Acknowledgments

We thank Xiao-Gang Wen, Yu-Peng Wang, Guang-Ming Zhang, and Jun-Peng Cao for helpful discussions. This work is supported by the Direct grant of CUHK (A/C 2060344) and NSFC.

-
- [1] H. T. Quan, Z. Song, X. F. Liu, P. Zanardi, and C. P. Sun, Phys. Rev. Lett. **96**, 140604 (2006).
 - [2] P. Zanardi and N. Paunkovic, Phys. Rev. E **74**, 031123 (2006).
 - [3] P. Zanardi, M. Cozzini, and P. Giorda, arXiv: quant-ph/0606130; M. Cozzini, P. Giorda, and P. Zanardi, Phys. Rev. B **75**, 014439 (2007); M. Cozzini, R. Ionicioiu, and P. Zanardi, arXiv: cond-mat/0611727.
 - [4] P. Buonsante and A. Vezzani, Phys. Rev. Lett. **98**, 110601 (2007).
 - [5] P. Zanardi, H. T. Quan, X. Wang, and C. P. Sun, Phys. Rev. A **75**, 032109 (2007).
 - [6] P. Zanardi, H. T. Quan, X. G. Wang, and C. P. Sun, Phys. Rev. A **75**, 032109 (2007).
 - [7] P. Zanardi, P. Giorda, and M. Cozzini, Phys. Rev. Lett. **99**, 100603 (2007).
 - [8] W. L. You, Y. W. Li, and S. J. Gu, Phys. Rev. E **76**, 022101 (2007).
 - [9] H. Q. Zhou and J. P. Barjaktarevic, arXiv: cond-mat/0701608; H. Q. Zhou, J. H. Zhao, and B. Li, arXiv:0704.2940;
 - [10] L. C. Venuti and P. Zanardi, Phys. Rev. Lett. **99**, 095701 (2007).
 - [11] S. Chen, L. Wang, S. J. Gu, and Y. Wang, Phys. Rev. E **76** 061108 (2007); S. Chen, L. Wang, Y. Hao, and Y. Wang, arXiv:0801.0020.
 - [12] S. J. Gu, H. M. Kwok, W. Q. Ning, and H. Q. Lin, arXiv:0706.2495.
 - [13] M. F. Yang, Phys. Rev. B **76**, 180403 (R) (2007); Y. C. Tzeng and M. F. Yang, Phys. Rev. A **77**, 012311 (2008).
 - [14] N. Paunkovic, P. D. Sacramento, P. Nogueira, V. R. Vieira, and V. K. Dugaev, arXiv:0708.3494.

- [15] H. Q. Zhou, R. Orus, and G. Vidal, *Phys. Rev. Lett.* **100** 080601 (2008).
- [16] A. Hamma, W. Zhang, S. Haas, and D. A. Lidar, arXiv:0705.0026.
- [17] M. A. Nilesen and I. L. Chuang, *Quantum Computation and Quantum Information* (Cambridge University Press, Cambridge, England, 2000).
- [18] S. Sachdev, *Quantum Phase Transitions* (Cambridge University Press, Cambridge, England, 1999).
- [19] X. G. Wen, *Quantum Field Theory of Many-Body Systems* (Oxford University, New York, 2004).
- [20] J. M. Kosterlitz and D. J. Thouless, *J. Phys. C* **6**, 1181(1973).
- [21] A. Kitaev, *Ann. Phys.* **303**, 2 (2003); *Ann. Phys.* **321**, 2 (2006).
- [22] X. G. Wen, *Phys. Rev. Lett.* **90**, 016803 (2003); M. A. Levin and X. G. Wen, *Phys. Rev. B* **71**, 045110 (2005).
- [23] J. Preskill, *Topological quantum computation*, <http://www.theory.caltech.edu/people/preskill/ph229/> (2004).
- [24] J. K. Pachos, *IJQI* **4**, 947 (2006); *Ann. Phys.* **322**, 1254 (2007).
- [25] S. D. Sarma, M. Freedman, C. Nayak, S. H. Simon, A. Stern, arXiv: 0707.1889.
- [26] X. Y. Feng, G. M. Zhang, and T. Xiang, *Phys. Rev. Lett.* **98**, 087204 (2007); D. H. Lee, G. M. Zhang, and T. Xiang, *Phys. Rev. Lett.* **99**, 196805 (2007).
- [27] H. D. Chen and J. P. Hu, arXiv: cond-mat/0702366; H. D. Chen and Z. Nussinov, arXiv: cond-mat/0703633; Z. Nussinov, G. Ortiz, arXiv: cond-mat/0702377.
- [28] Y. Yu, arXiv: 0704.3829; Y. Yu, Z. Q. Wang, arXiv: 0708.0631; T. Y. Si and Y. Yu, arXiv:0709.1302; T. Y. Si and Y. Yu, arXiv: 0712.4231 .
- [29] S. Yang, D. L. Zhou, and C. P. Sun, *Phys. Rev. B* **76**, 180404(R) (2007).
- [30] S. P. Kou and X. G. Wen, arXiv: 0711.0571.
- [31] S. Mandal and N. Surendran, arXiv: 0801.0229.
- [32] K. P. Schmidt, S. Dusuel, and J. Vidal, *Phys. Rev. Lett.* **100**, 057208 (2008); S. Dusuel, K. P. Schmidt, and J. Vidal, arXiv:0802.0379.
- [33] J. H. Zhao and H. Q. Zhou, arXiv:0803.0814.